Supporting Information for

Ethylene Tetramerization Catalysis: Effects of Aluminum-Induced Isomerization of PNP to PPN Ligands

Alejo M. Lifschitz, Nathanael A. Hirscher, Heui Beom Lee, Joshua A. Buss, and Theodor Agapie*

*To whom correspondence should be addressed, E-mail: agapie@caltech.edu.

Division of Chemistry and Chemical Engineering, California Institute of Technology, 1200 East California Boulevard MC 127-72, Pasadena, California 91125, United States

Table of Contents

Materials and Methods

All synthetic procedures and experiments were performed in a nitrogen-atmosphere glove box or in sealed containers under a stream of nitrogen gas. All glassware was oven-dried for 24 hours and kept under active vacuum for at least 8 hours prior to use. Dichloromethane (CH_2Cl_2), diethyl ether, tetrahydrofuran (THF), pentane and hexanes solvents were transferred from an oxygen- and water-free solvent system into sealed containers, degassed under active vacuum and stored over activated molecular sieves for 1 day prior to use. Deuterated benzene (Cambridge Isotope Laboratories) and toluene (used for catalytic experiments) were dried over Na/benzophenone, vacuum distilled and kept over activated molecular sieves prior to use. Deuterated CD_2Cl_2 was dried over CaH_2, vacuum distilled and kept over activated molecular sieves prior to use. The syntheses of compounds **1**,[1] **2**,[2] and **13**[3] have been previously reported. $AlMe_3$ and $AlClMe_2$ (0.9 M in heptane) were purchased from Aldrich Chemical Co. M-MAO 3A was purchased from AkzoNobel as a 7% w/w Al solution in heptane. Anhydrous $AlCl_3$ was purchased from Alfa Aesar as 99.998% grade. All other chemicals were purchased from Aldrich Chemical Co. and dried under active vacuum overnight prior to use. NMR spectra were recorded on a Varian Spectrometer. ^1H and ^{13}C NMR spectra were referenced to solvent resonances. $^{31}P\{^1H\}$ NMR spectra were referenced to an 85% H_3PO_4 aqueous solution. All chemical shifts are reported in ppm.

Ethylene Oligomerization

Ethylene oligomerization experiments were carried out in a Fisher-Porter vessel equipped with a metal top regulator. The oven-dried Fisher-Porter vessel and the metal top regulator were kept under active vacuum overnight prior to setup in the glovebox. In a nitrogen-atmosphere

glove box, 8 μmol of $CrCl_3(THF)_3$ and 8 μmol of phosphine ligand were dissolved in 10 mL of toluene and added to the Fisher-Porter vessel (precatalyst concentration: 0.8 mM). The Fisher-Porter vessel was then sealed and it was connected to an ethylene line outside the glove box. The ethylene feed was purified through a Matheson TriGas oxygen/moisture purifying column. The Fisher-Porter setup was purged with ethylene at 60 psi for 2 minutes and the pressure was then reduced to 20 psi. Under vigorous stirring, the MMAO solution was injected through a rubber septum and the pressure was increased to 60 psi. In all cases, the final reaction volume after injection of the activator or activator solution was 10 mL. The setup was kept at 25 ˚C for 1 hour, after which the reactor was depressurized and 10 mg of adamantane standard were added. The activator was quenched via the addition of 20 mL of 1M $HCl_{(aq)}$ and the organic portion was filtered through a pad of basic alumina. The amount of oligomers produced was determined via GC and the polymer was isolated via vacuum filtration over a fritted funnel and dried under active vacuum for 24 hours.

X-Ray Crystallography

Suitable crystals were mounted on a nylon loop using Paratone oil, then placed on a diffractometer under a nitrogen stream. X-ray intensity data were collected on a Bruker APEXII CCD area detector or a Bruker D8 VENTURE Kappa Duo PHOTON 100 CMOS detector employing Mo-Kα radiation (λ = 0.71073 Å) at a temperature of 100 K. All diffractometer manipulations, including data collection, integration and scaling were carried out using the Bruker APEX3 software. Frames were integrated using SAINT. The intensity data were corrected for Lorentz and polarization effects and for absorption using SADABS. Space groups were determined on the basis of systematic absences and intensity statistics using XPREP. Using Olex2, the structures were solved by direct methods using ShelXT and refined to convergence by

full-matrix least squares minimization using ShelXL. All non-hydrogen atoms were refined using anisotropic displacement parameters. Hydrogen atoms were placed in idealized positions and refined using a riding model. For complex **7b/7c**, the substitutional disorder at C1 and Cl1 was modeled using the PART instruction. For complex **11**, the positional disorder of the $OAlCl_3$ moiety was modeled using the PART instruction. For complex **12**, the substitutional disorder of the $[AlCl_4]^-$ and the $[AlCl_3Me]^-$ anions was modeled using the PART instruction.

Procedures

$[CrCl_3(1)]_2$ (**3**). $CrCl_3(THF)_3$ (200 mg, 0.27 mmol) was suspended in CH_2Cl_2 (5 mL) and a solution of **1** (254 mg, 0.54 mmol) in CH_2Cl_2 (5 mL) was added in a dropwise fashion over 5 minutes. The solution turned blue-green and was left to stir overnight. The solvent was then removed in vacuo yielding a blue-green solid. The residue was redissolved in CH_2Cl_2 (1.5 mL) and the product was obtained as purple crystals from vapor diffusion of pentane into the CH_2Cl_2 solution. ^{1}H NMR (400.16 MHz, 25˚C, C_6D_6): δ 13.79 (br s), 10.60 (br s), 7.46 (s), 6.93 (s), 6.02 (br s), 4.20 (s), 3.55 (s), 1.96 (br s), 1.29 (br m), 0.82 (s), 0.25 (s), -0.88 (br s). ^{31}P{^{1}H} NMR (162.0 MHz, 25˚C, C_6D_6): silent. μ_{eff} = 5.4 μ_B. Anal. Calcd for $C_{62}H_{55}Cl_6Cr_2N_2P_4$: C, 58.70; H, 4.37; N, 2.21. Found: C, 59.05; H, 5.56; N, 1.97.

$[CrCl_3(2)]_2$ (**4**). $CrCl_3(THF)_3$ (200 mg, 0.27 mmol) was suspended in toluene (5 mL) and a solution of **2** (228 mg, 0.54 mmol) in toluene (5 mL) was added in a dropwise fashion over 5 minutes. The solution turned blue and was left to stir overnight. The solvent was then removed in vacuo yielding a blue-purple solid. The residue was redissolved in CH_2Cl_2 (1.5 mL) and the product was obtained as blue-purple crystals from vapor diffusion of pentane into the CH_2Cl_2 solution. ^{1}H NMR (400.16 MHz, 25˚C, CD_2Cl_2): δ 15.35 (br s), 11.94 (br s), 10.59 (br s), 7.95-

7.15 (m), 4.75-2.75 (m), 2.36 (s), 1.30-0.90 (m), 0.10 (s), -0.29 (br s). $^{31}P\{^{1}H\}$ NMR (162.0 MHz, 25˚C, CD_2Cl_2): silent. μ_{eff} = 5.4 μ_B. Anal. Calcd for $C_{54}H_{55}Cl_6Cr_2N_2P_4$: C, 55.31; H, 4.73; N, 2.39. Found: C, 55.08; H, 4.82; N, 2.27.

(*p*-tol)PNP-AlMe$_3$ (5). Phosphine **1** (0.040 g, 0.084 mmol) and $AlMe_3$ (0.055 g, 0.38 mmol) were mixed in 2 mL toluene. After 30 minutes, the colorless solution was transferred to a tared vial and reduced in vacuo to a sticky residue, redissolved in C_6H_6, and reduced to dryness in vacuo again. The remaining white solids were triturated with hexanes to yield the product as a white powder (0.045 g, 85% yield). ^{1}H NMR (399.8 MHz, 23˚C, C_6D_6): 7.55 (m, 8H), 7.04 (m, 12H), 6.60 (d, J_{H-H} = 7.8 Hz, 2H), 6.51(d, J_{H-H} = 7.8 Hz, 2H), 1.84 (s, 3H), -0.23 (s, 9H).). ^{31}P NMR (121.38 MHz, 25˚C, C_6D_6): 64.92 (s). $^{13}C\{^{1}H\}$ NMR (100.54 MHz, 25˚C, C_6D_6): δ 140.6 (s), 136.7 (s), 135.4, 134.2 (t, J_{P-C} = 10.0 Hz), 130.8, 130.4, 129.3, 128.53 (m), 20.7 (s), -7.2 (s). Anal. Calcd for $C_{34}H_{36}AlNP_2$: C, 74.58; H, 6.63; N, 2.56. Found: C, 74.65; H, 6.64; N, 2.36.

(*p*-tol)PPN-AlClMeX (84 % 7a: X = Me; 16% 7b: X = Cl). Phosphine **1** (150 mg, 0.32 mmol) was dissolved in toluene (5 mL) and 0.70 mL of a 0.9 M $AlClMe_2$ solution in heptane (2 equiv., 0.64 mmol) were added in a dropwise fashion. After stirring overnight, the solvent was removed in vacuo and the white solids were redissolved in 2 mL of CH_2Cl_2. The product was obtained as colorless crystals via vapor diffusion of pentane into the CH_2Cl_2 solution (isolated yield 154 mg, 86%). Quantitative assignment of Cl/Me substitution on Al for 7a versus 7b is based on the ratios of ^{1}H NMR resonances at -1.13 and -1.29 ppm and ^{31}P resonances. In the ^{13}C spectrum, Al-*C*H_3 resonances for 7a and 7b overlap at -6.1 ppm, as do all other resonances in the ^{13}C and ^{1}H spectra. ^{1}H NMR (400.16 MHz, 25˚C, CD_2Cl_2): δ 7.74 (m, 6 H), 7.60 (d, J_{H-H} = 4 H), 7.31 (m, 2 H), 7.08 (m, 4 H), 6.98 (m, 2 H), 6.65 (m, 6 H), 2.20 (s, 3 H), -1.13 (s, 0.5 H, $AlCl_2CH_3$), -1.29

(s, 5 H, AlCl(C*H*$_3$)$_2$). ^{31}P{^{1}H} NMR (162.0 MHz, 25˚C, CD_2Cl_2): δ 37.2 (d, $J_{P\text{-}P}$ = 293 Hz, **7a**), 39.5 (d, $J_{P\text{-}P}$ = 297 Hz, **7b**), -10.3 (d, $J_{P\text{-}P}$ = 297 Hz, **7b**), -10.6 (d, $J_{P\text{-}P}$ = 293 Hz, **7a**). ^{13}C{^{1}H} NMR (100.54 MHz, 25˚C, CD_2Cl_2): δ 139.6 (s), 136.2 (s), 135.2, 135.1, 134.4, 133.9, 131.8, 131.5, 130.7, 129.3, 129.2, 128.8, 127.7 (s), 127.0 (m), 20.9 (s), -6.1 (s).

(*i*-Pr)PNP-Al$_2$Cl$_3$Me$_3$ (**8**). Phosphine **2** (125 mg, 0.29 mmol) was dissolved in toluene (5 mL) and 0.98 mL of a 0.9 M $AlClMe_2$ solution in heptane (3 equiv., 0.88 mmol) were added in a dropwise fashion. The solution was stirred at room temperature for 2 days and the solvent was removed in vacuo. The resulting white solid was redissolved in minimal CH_2Cl_2 and the product was obtained as clear crystals via vapor diffusion of pentane (isolated yield 172 mg, 92%). ^{1}H NMR (300.08 MHz, 25˚C, C_6D_6): δ 7.57 (m, 8 H), 7.06 (m, 12 H), 3.74 (hept, $J_{H\text{-}H}$ = 6.2 Hz, 1 H), 1.03 (d, $J_{H\text{-}H}$ = 6.6 Hz, 6 H), -0.21 (br m, 9 H). ^{31}P{^{1}H} NMR (121.48 MHz, 25˚C, C_6D_6): δ 53.6 (br s). ^{13}C{^{1}H} NMR (100.54 MHz, 25˚C, C_6D_6): δ 137.7 (s), 133.1 (d, $J_{C\text{-}P}$ = 26.4 Hz), 129.2 (s), 128.1 (d, $J_{C\text{-}P}$ = 7.5 Hz), 67.1 (s), 53.0 (s), 24.2 (s), 12.9 (s). Anal. Calcd for $C_{30}H_{36}Al_2Cl_3NP_2$: C, 56.93; H, 5.73; N, 2.21. Found: C, 56.65; H, 5.78; N, 2.23.

(*i*-Pr)PNP-H AlCl$_4$ (**10$^+$[AlCl$_4$]$^-$**). A solution of phosphine **2** (125 mg, 0.29 mmol) in CH_2Cl_2 (5 mL) was added in a dropwise fashion to a $AlCl_3$ (2 equiv., 78.1 mg, 0.59 mmol) suspension in toluene (2 mL). 1 equiv. of H_2O (5.2 μL) were injected through a rubber septum and the mixture was stirred for 1 day. The volatiles were then removed and the resulting white solid was dissolved in minimal CH_2Cl_2. The product was obtained as colorless crystals via vapor diffusion of pentane into the CH_2Cl_2 solution (isolated yield 86 mg, 48%). ^{1}H NMR (399.8 MHz, 25˚C, CD_2Cl_2): δ 8.47 (dd, $J_{H\text{-}P}$ = 14.3, 518 Hz, 1H), 7.88 (t, $J_{H\text{-}H}$ = 7.0 Hz, 2H), 7.72-7.37 (m, 18 H), 4.06 (m, 1 H), 1.39 (d, $J_{H\text{-}H}$ = 6.7 Hz, 6 H). ^{31}P{^{1}H} NMR (161.85 MHz, 25˚C, CD_2Cl_2): δ 52.3 (d, $J_{P\text{-}P}$ = 11.7 Hz, 1 P), 21.4 (d, $J_{P\text{-}P}$ = 11.7 Hz, 1 P). ^{13}C{^{1}H} NMR (100.54 MHz, 25˚C,

CD_2Cl_2): δ 136.5 (s), 133.8 (d, J_{C-P} = 12.7 Hz), 133.3 (dd, J_{C-P} = 3.7, 15.3 Hz), 133.0 (d, J_{C-P} = 21.3 Hz), 131.7 (s), 130.9 (d, J_{C-P} = 14.0 Hz), 130.0 (d, J_{C-P} = 6.8 Hz), 118.7 (d, J_{C-P} = 98.2 Hz), 53.9 (s), 23.8 (s). HRMS Calc. for $[M\text{-}AlCl_4]^+$: 428.1697. Found: 428.1672. Anal. Calcd for $C_{27}H_{28}AlCl_4NP_2$: C, 54.30; H, 4.73; N, 2.35. Found: C, 53.45; H, 4.22; N, 2.30.

PPO $AlCl_3$ (11). A solution of phosphine **2** (125 mg, 0.29 mmol) in THF (5 mL) was added in a dropwise fashion to a $AlCl_3$ (1 equiv., 39 mg, 0.29 mmol) in THF (2 mL). 1 equiv. of H_2O (5.2 μL) were injected through a rubber septum and the mixture was stirred for 2 days. The solvent was then removed in vacuo, the resulting white residue redissolved in CH_2Cl_2, and the crude product was precipitated out of solution via addition of pentane. From the resulting mixture, colorless crystals suitable for single crystal XRD were grown via vapor diffusion of pentane into a solution of the crude white powder in CH_2Cl_2.

$[Cr_2(p\text{-tol-PNP})_2Cl_3Me_2]AlCl_4$ (12). Complex **3** (50 mg, 0.039 mmol) was dissolved in toluene (10 mL) and the solution was frozen. As the solution was thawing, a 0.9 M solution of $AlCl_2Me$ in heptane (9 μL, 2 equiv., 0.078 mmol) were added. The solution turned green upon warming to room temperature and it was left to stir at room temperature for 2 hours. The solvent was then reduced to approximately 1 mL and the product was crystalized via vapor diffusion of pentane into the toluene solution (isolated yield 39 mg, 83%). The complex was observed to degrade room temperature, which was evidenced by a change in color and a deviation from the expected values in the elemental analysis. ^1H NMR (400.16 MHz, 25˚C, C_6D_6): δ 11.79 (br m), 8.94 (br m), 7.90-5.80 (br m), 4.26 (br s), 3.54 (br m), 2.80-0.80 (br m), 0.00- –0.90 (br m). $^{31}P\{^1H\}$ NMR (162.0 MHz, 25˚C, C_6D_6): silent. μ_{eff} = 5.5 μ_B. Anal. Calcd for $C_{64}H_{60}AlCl_7Cr_2N_2P_4$: C, 56.51; H, 4.45; N, 2.06. Found: C, 57.42; H, 4.78; N, 1.83.

$Ph_2PN(p\text{-}tol)Li\cdot THF$ (14). (N-diphenylphosphino)-p-toluidine (300 mg, 1.03 mmol) was dissolved in 10 mL THF and the solution was cooled to -78 ˚C. A 2.5 M solution of n-BuLi in hexanes (0.41 mL, 2 equiv., 1.0 mmol) was added in a dropwise fashion via a rubber septum. After stirring for 30 minutes, the solution was allowed to warm up to room temperature and it was stirred for a further 60 minutes. The solvent was removed in vacuo and the resulting yellow sticky solid was triturated with pentane to give the product as a light yellow powder containing 1 equiv. of THF as quantified by ^{1}H NMR after pumping down the solids in vacuo for 4 hours (isolated yield: 362 mg, 98%). Colorless solid precipitate was observed to form from yellow MeCN solutions after about an hour, with only a slight shift in ^{1}H and ^{31}P resonances. ^{1}H NMR (399.8 MHz, 25˚C, CD_3CN): δ 7.52-7.41 (m, 4 H), 7.39-7.27 (m, 6 H), 6.91-6.78 (m, 4H), 3.65 (m, 4H), 2.17 (s, 3H), 1.80 (m, 4H). ^{31}P{^{1}H} NMR (161.9 MHz, 25˚C, CD_3CN): δ 30.8 (s). ^{13}C{^{1}H} NMR (125.7 MHz, 25˚C, CD_3CN): δ 145.5 (d, J = 17.6 Hz), 141.4 (d, J = 12.2 Hz), 131.9 (d, J = 20.2 Hz), 130.5 (s), 129.9 (s), 129.4 (d, J =6.4 Hz), 129.1 (s), 116.9 (d, J = 12.3 Hz), 68.3 (s), 26.2 (s), 20.4 (s). Anal. Calcd for $C_{23}H_{25}LiNOP$: C, 74.79; H, 6.82; N, 3.79. Found: C, 74.04; H, 7.36; N, 3.61.

Procedures for Reactions with PNP Ligands

Representative Cyclam Quenching Procedure (Figure S8-S9): To a stirring solution of **1** (10 mg) and $CrCl_3(THF)_3$ (8 mg, 1 equiv.) in toluene (0.5 mL), a prepared solution of $AlMe_3$ (0.5 mL, 0.2 M in toluene, 4 equiv.) was added. The solution changed color from blue to green. After 1 hour, the oily green suspension was used to dissolve cyclam (13 mg, 3 equiv.) and a brown solution was filtered from purple solids both immediately and after an addition 2 hours. The peak at 69 ppm corresponds to **1**. The peak at 29 ppm corresponds to $Ph_2PN(tol)H$ or Al-bound $Ph_2PN(tol)$ (Figure S19). The peak at -27 ppm corresponds to Ph_2PMe (Figure S20).

Representative Hydrolysis of MMAO Procedure (Figure S10-S11): To a stirring solution of **1** (5.0 mg) in toluene (1 mL), MMAO-3A was added (0.06 mL, 10 equiv.) in the glovebox. The solution was added to a septum-capped NMR tube, and outside the glovebox, H_2O (10 equiv.) was added via a microsyringe. A significant amount of solid precipitate formed in the NMR tube, and soluble species in the tube were monitored over time via ^{31}P NMR. The peak at 69 ppm corresponds to **1**. The peak at 29 ppm corresponds to $Ph_2P(O)Me$, as opposed to Al-bound $Ph_2PN(tol)$. The sample was divided into two portions and separately spiked with an authentic sample of $Ph_2P(O)Me$ and $Ph_2PN(tol)Li\cdot$ THF. Only in the former case did the resonance at 29 ppm grow in to overlap perfectly with the additive. The peak at -27 ppm corresponds to Ph_2PMe (Figure S20).

MeMgBr Reaction with 7 (Figure S15): To a stirring solution of solution of **1** (22 mg) in toluene (1 mL), $AlMe_2Cl$ (2 equiv.) was added. After 4 days, MeMgBr (1 equiv. in Et_2O) was added, causing precipitate within seconds (magnesium salts). The soluble species were monitored over time via ^{31}P NMR. The peak at 69 ppm corresponds to **1** (25%). The peak at 29 ppm (<1%) is assigned to Al-bound or Mg-bound $Ph_2PN(tol)$, although some of these species may have precipitated out (Figure S19). The peak at -26 ppm corresponds to Ph_2PMe (Figure S20) (7%). Unreacted 7 is present (63%), as well as an additional PPN species (32 ppm, -12 ppm, 4%) that is not assigned. In a control experiment, addition of 2 equiv. $AlMe_2Cl$ to **12**, followed by 1 equiv. MeMgBr, showed no degradation of the peak at 30 ppm (Al-bound PN species) over 20 hours. Furthermore, addition of MeMgBr to **1** in toluene, in a separate control experiment, showed no degradation of **1** after 16 hours.

$AlMe_3$ Reaction with 7 (Figure S15): To a stirring solution of solution of **1** (22 mg) in toluene (1 mL), $AlMe_2Cl$ (2 equiv.) was added. After 4 days, $AlMe_3$ (50 equiv. in 0.5 mL toluene) was

added. The species in the homogeneous solution were monitored over time via ^{31}P NMR. The product with a resonance at 24 ppm (53%) is not assigned, but is also reproduced by reacting **12** with 2 $AlMe_2Cl$ followed by 50 $AlMe_3$, suggesting intermediacy of a PN species in the reaction (Figure S19). The peak at -11 ppm is not assigned (6%). The peak at -24 ppm corresponds to Al-bound Ph_2PMe (Figure S21) (41%).[4]

NMR Characterization

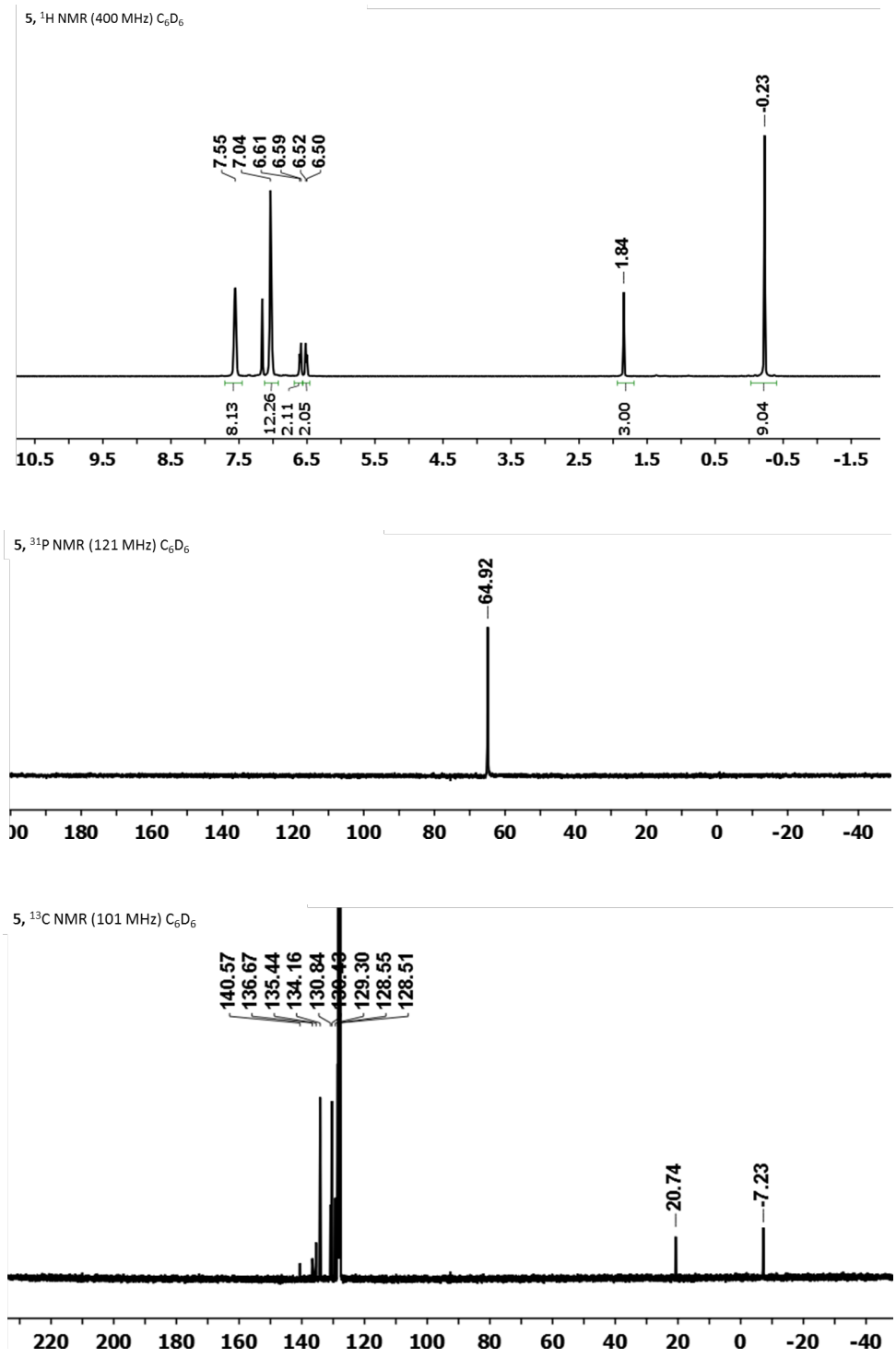

Figure S1. ^{1}H, ^{31}P{^{1}H} and ^{13}C{^{1}H} NMR spectra of compound **5**.

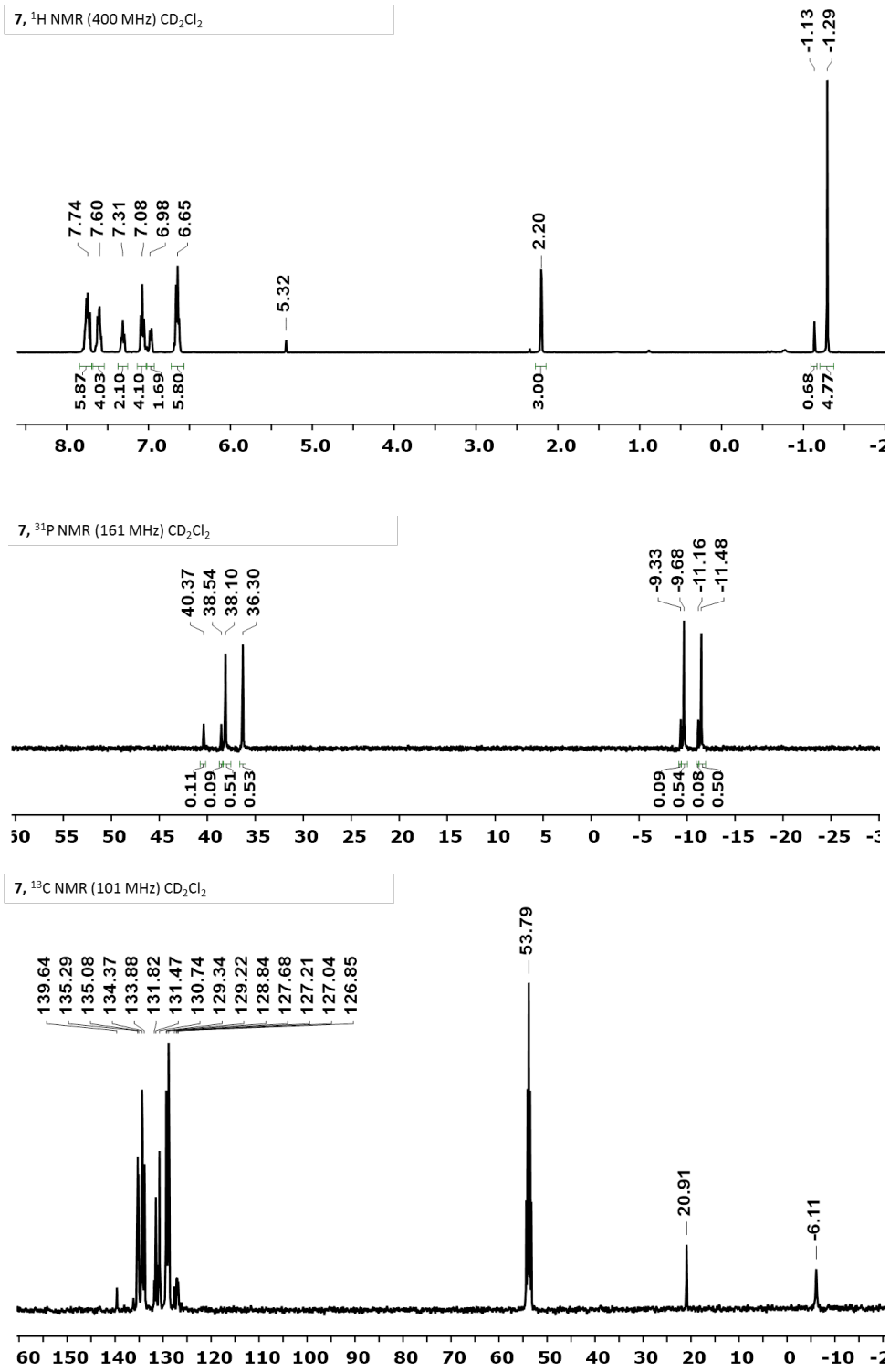

Figure S2. ^{1}H, ^{31}P{^{1}H} and ^{13}C{^{1}H} NMR spectra of compound **7**.

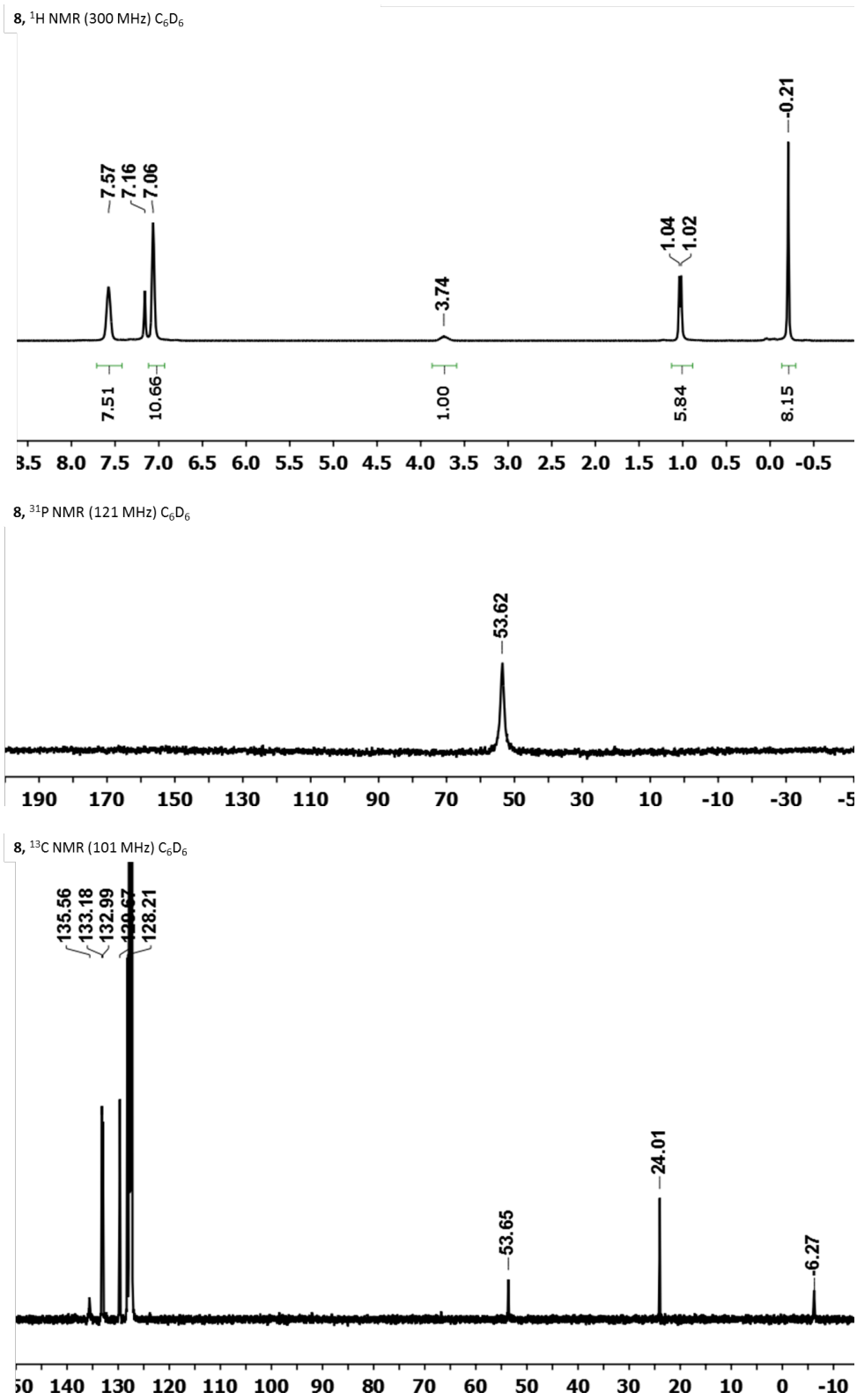

Figure S3. ^{1}H, ^{31}P{^{1}H} and ^{13}C{^{1}H} NMR spectra of compound **8**.

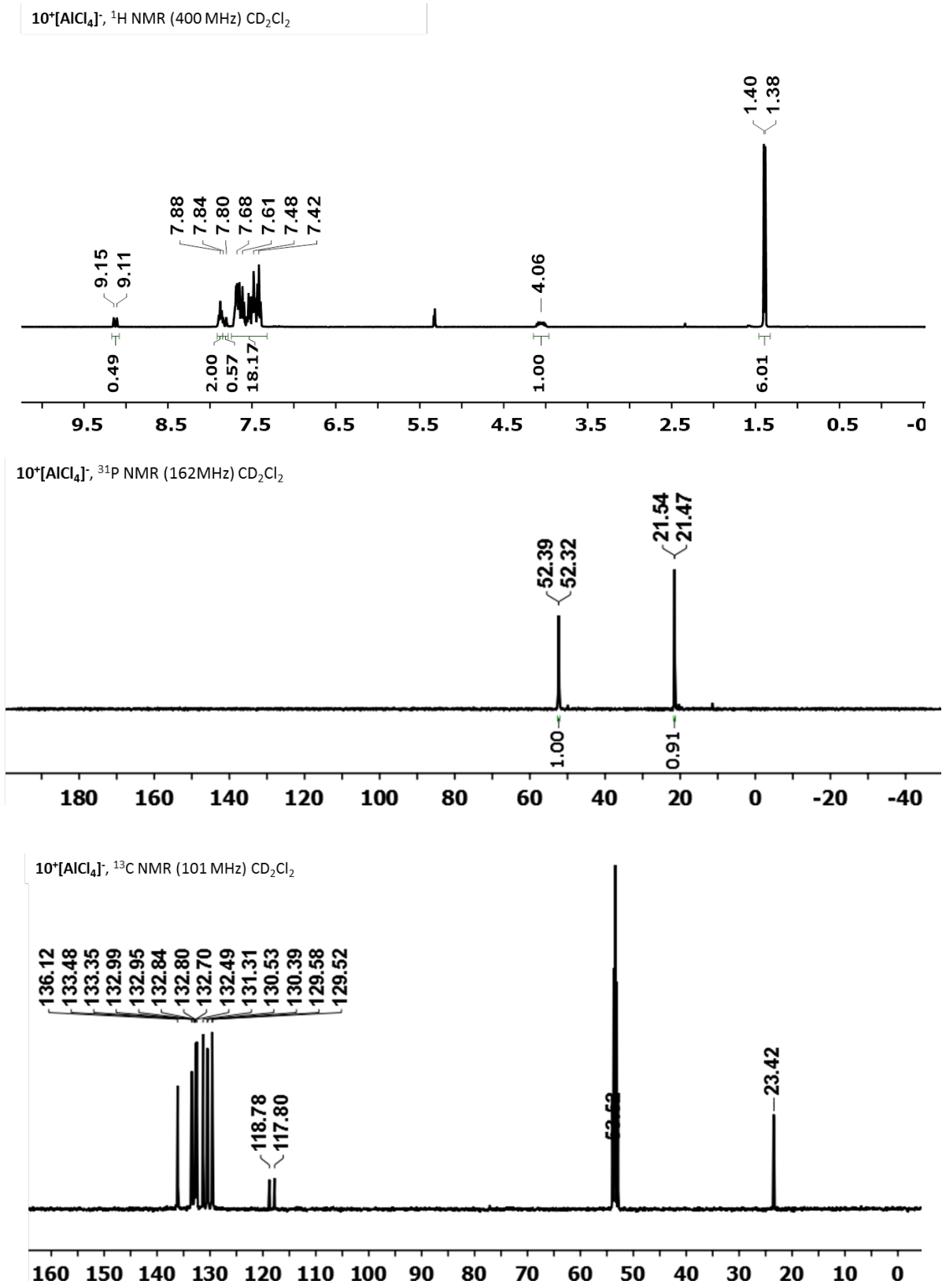

Figure S4. ^{1}H, $^{31}P\{^{1}H\}$ and $^{13}C\{^{1}H\}$ NMR spectra of compound $\mathbf{10^{+}[AlCl_4]^{-}}$.

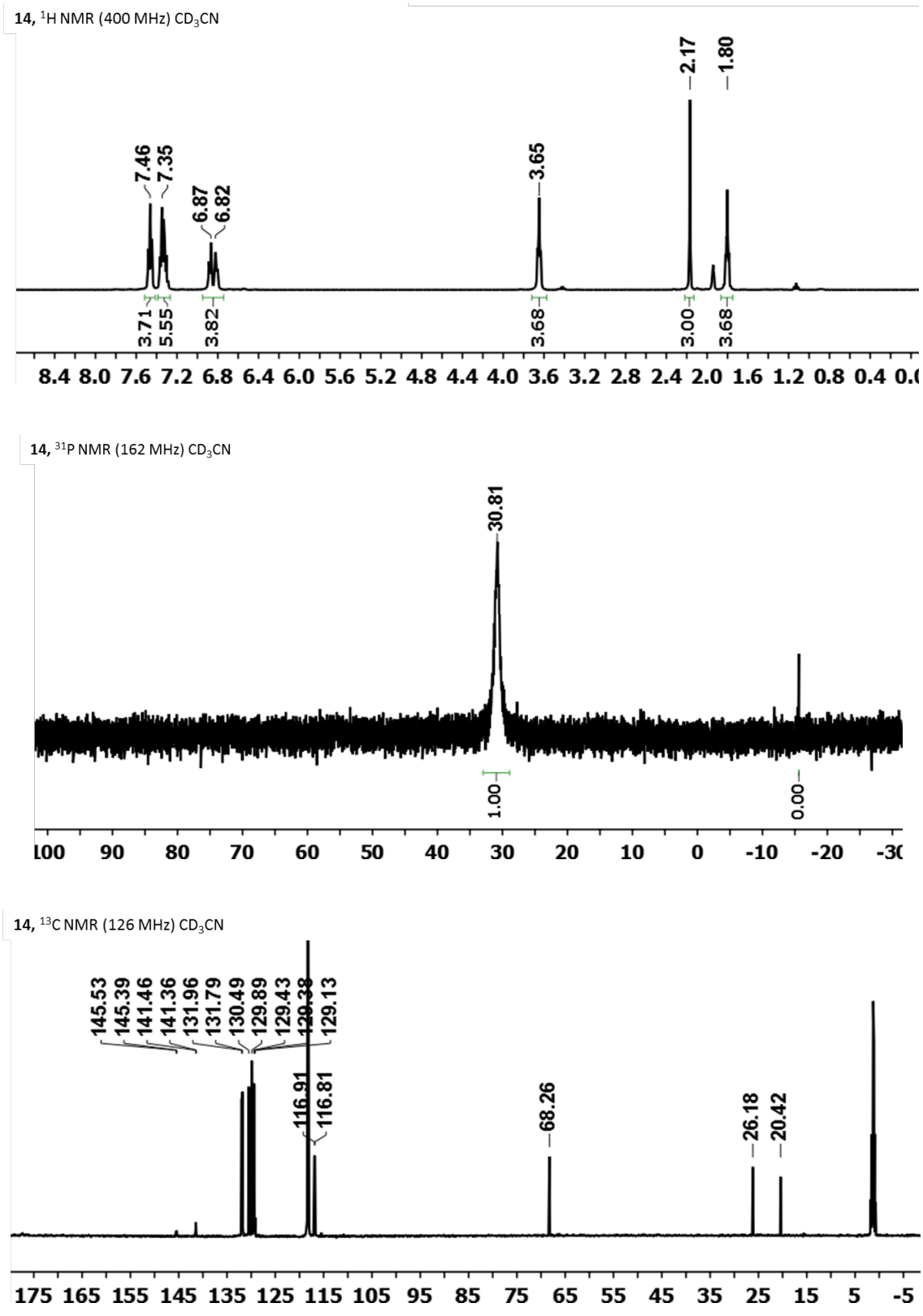

Figure S5. ^{1}H, ^{31}P{^{1}H} and ^{13}C{^{1}H} NMR spectra of compound **14**.

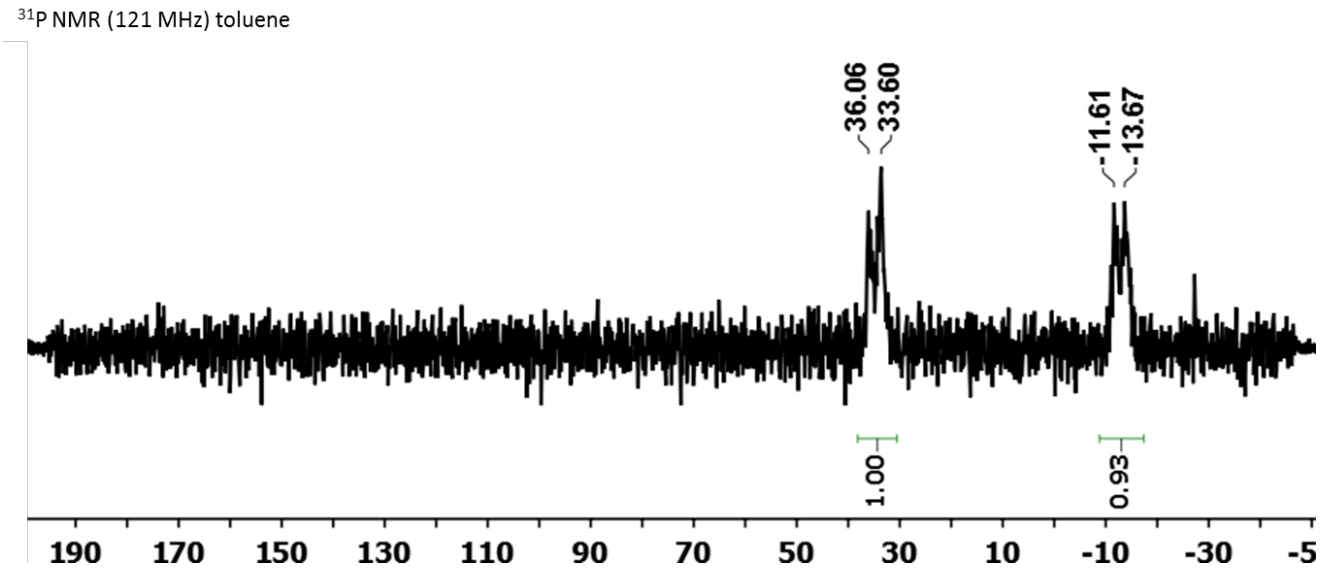

Figure S6. $^{31}P\{^{1}H\}$ NMR spectrum of $HBAr^{F}_{4}$ + **1** (**9**$^{+}$**[BAr′$_4$]**$^{-}$).

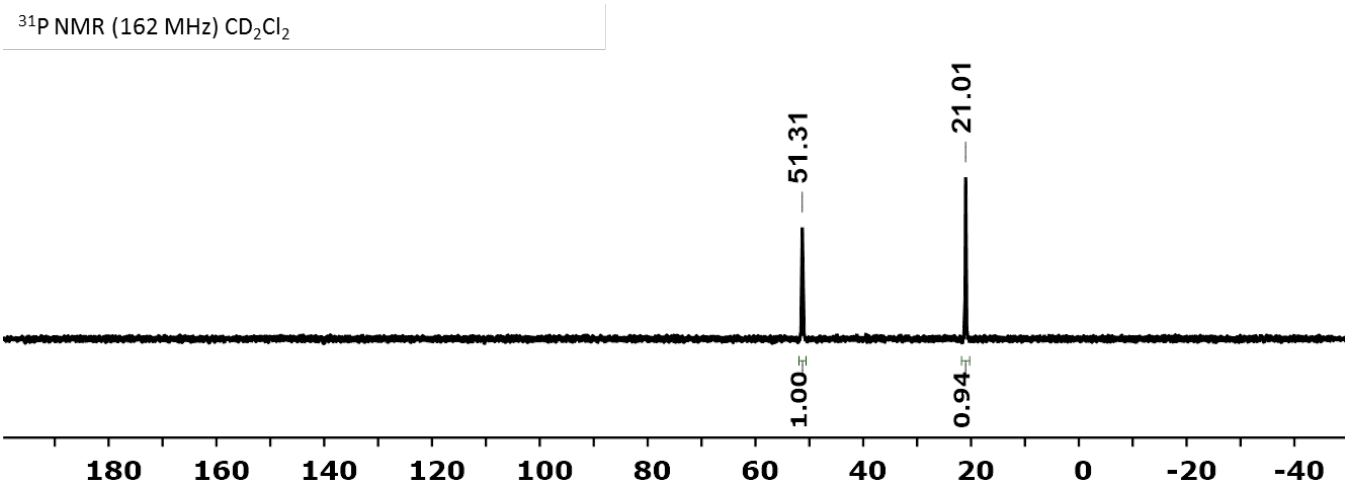

Figure S7. $^{31}P\{^{1}H\}$ NMR spectrum of $HBAr^{F}_{4}$ + **2** (**10**$^{+}$**[BAr′$_4$]**$^{-}$)

Cr Extraction under Activation Conditions

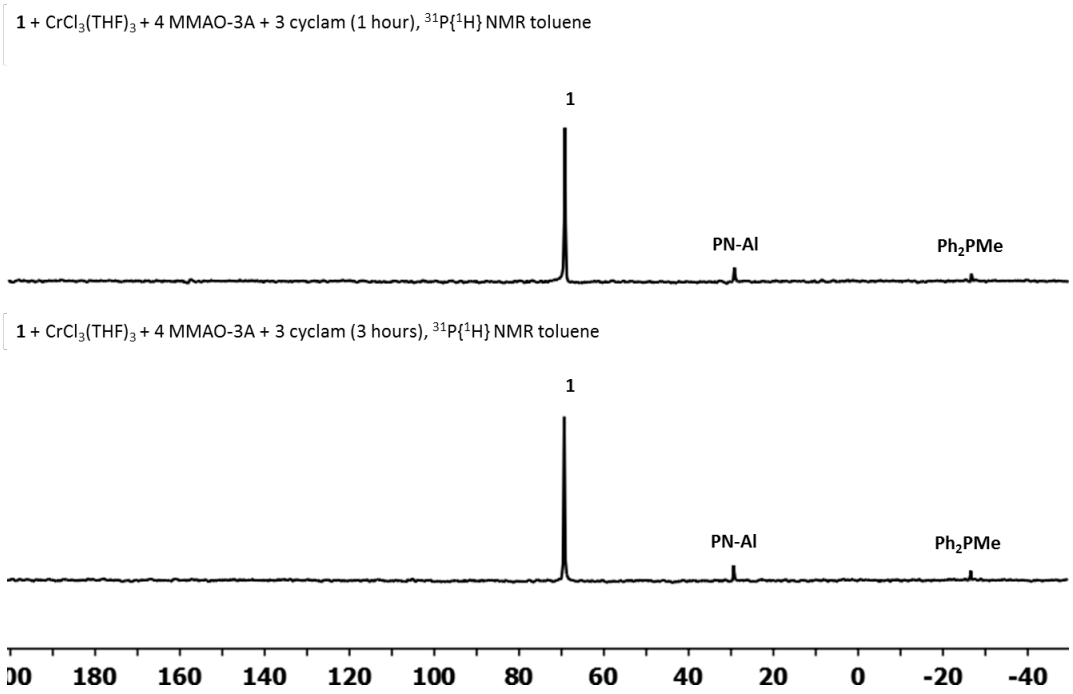

Figure S8. $^{31}P\{^1H\}$ NMR spectra of cyclam extraction of 4 MMAO-3A + **1** + $CrCl_3(THF)_3$.

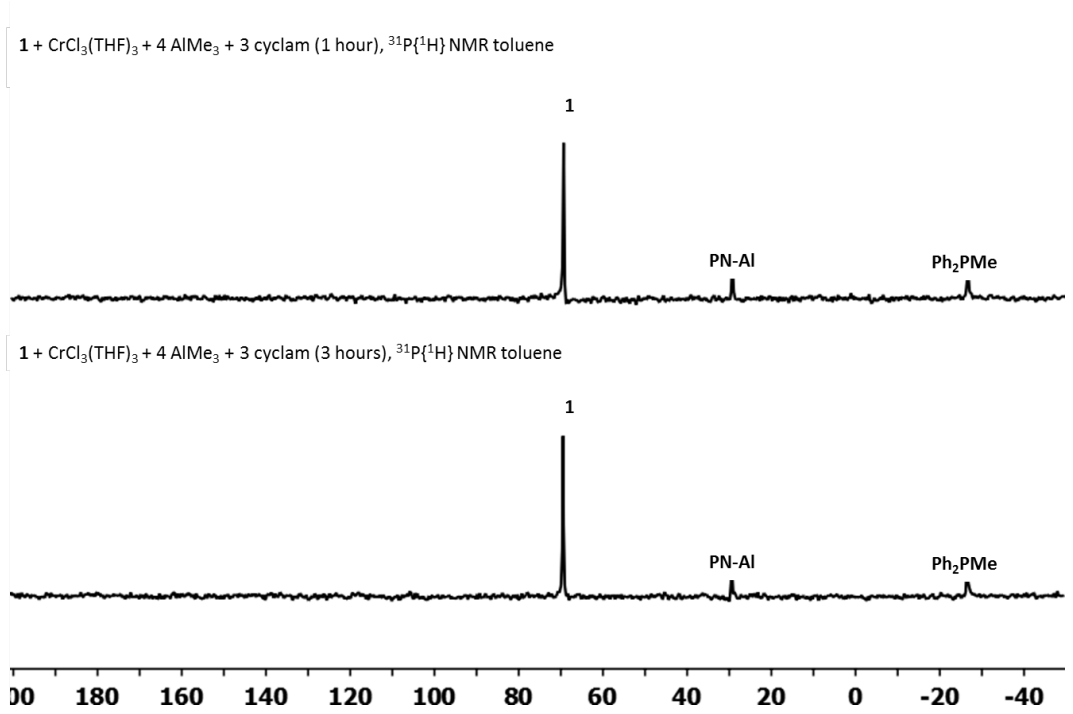

Figure S9. $^{31}P\{^1H\}$ NMR spectra of cyclam extraction of 4 $AlMe_3$ + **1** + $CrCl_3(THF)_3$.

PNP Reactivity with Hydrolyzed MMAO

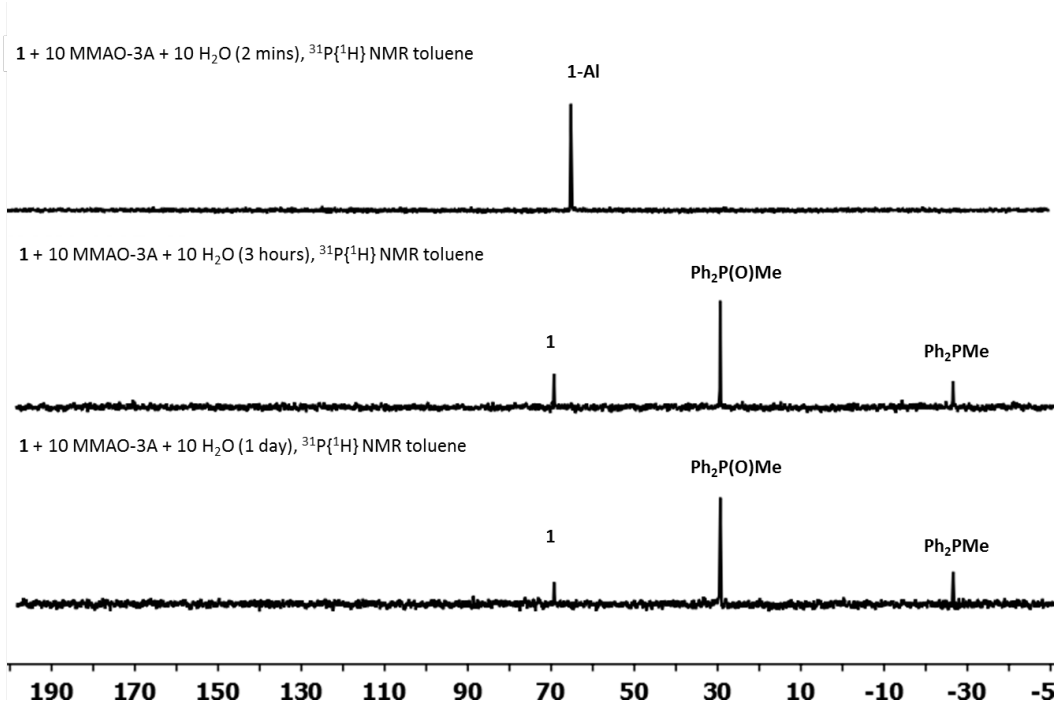

Figure S10. $^{31}P\{^{1}H\}$ NMR spectra of **1** + 10 MMAO-3A + 10 H_2O.

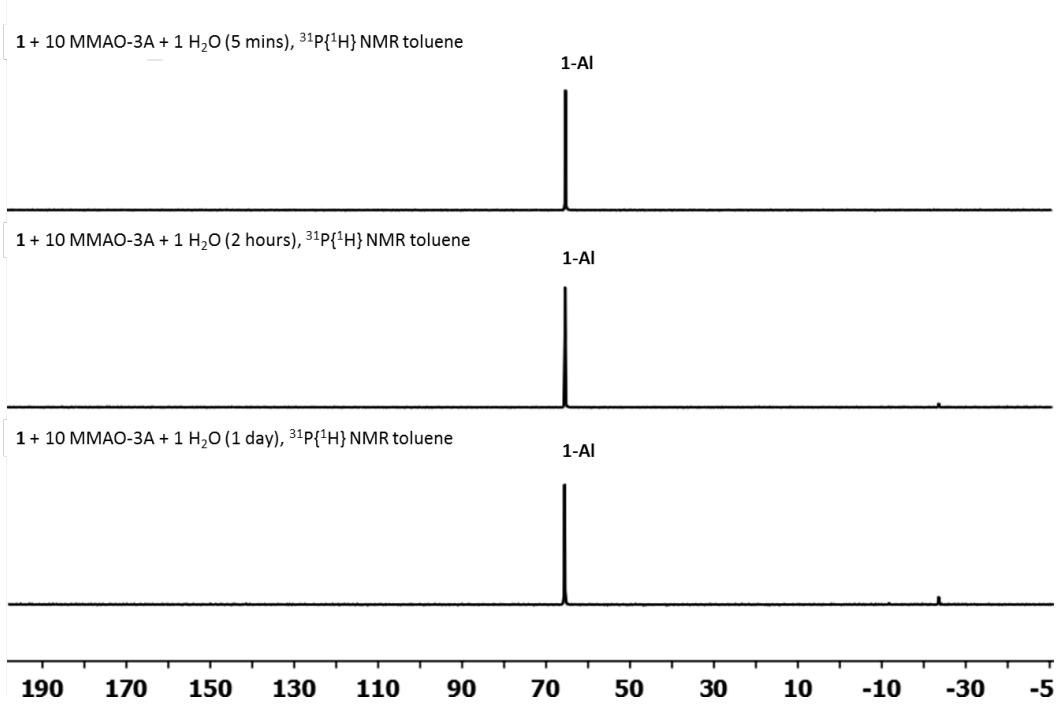

Figure S11. $^{31}P\{^{1}H\}$ NMR spectra of **1** + 10 MMAO-3A + 1 H_2O.

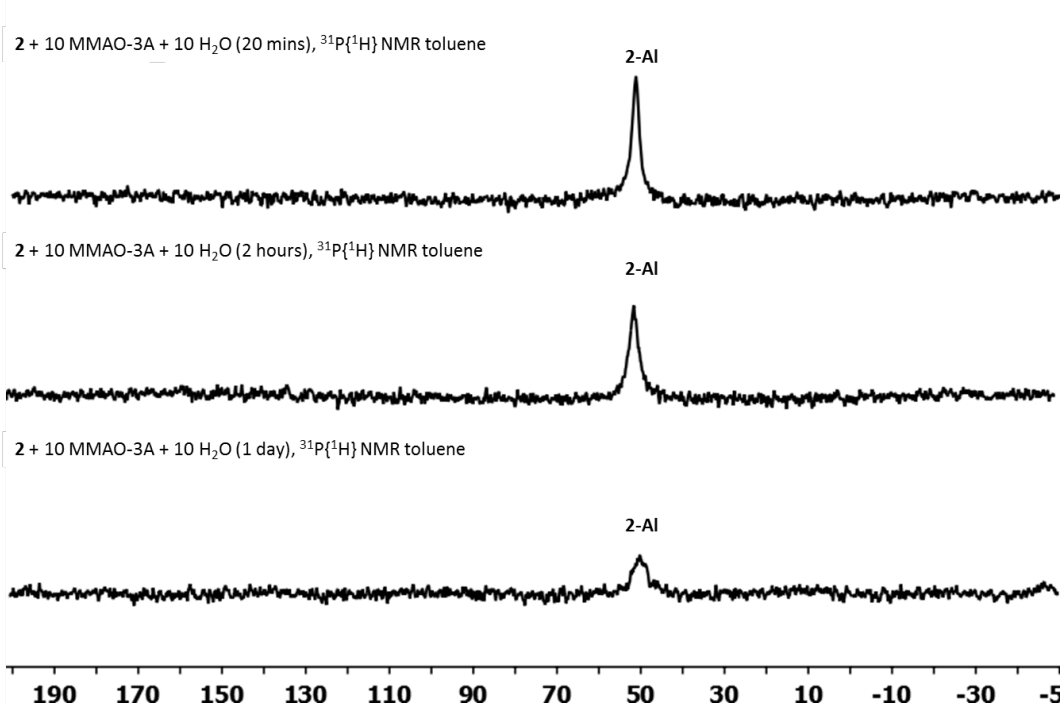

Figure S12. $^{31}P\{^{1}H\}$ NMR spectra of **2** + 10 MMAO-3A + 10 H_2O.

PNP Reactivity with Chlorinated Alkyl Aluminum

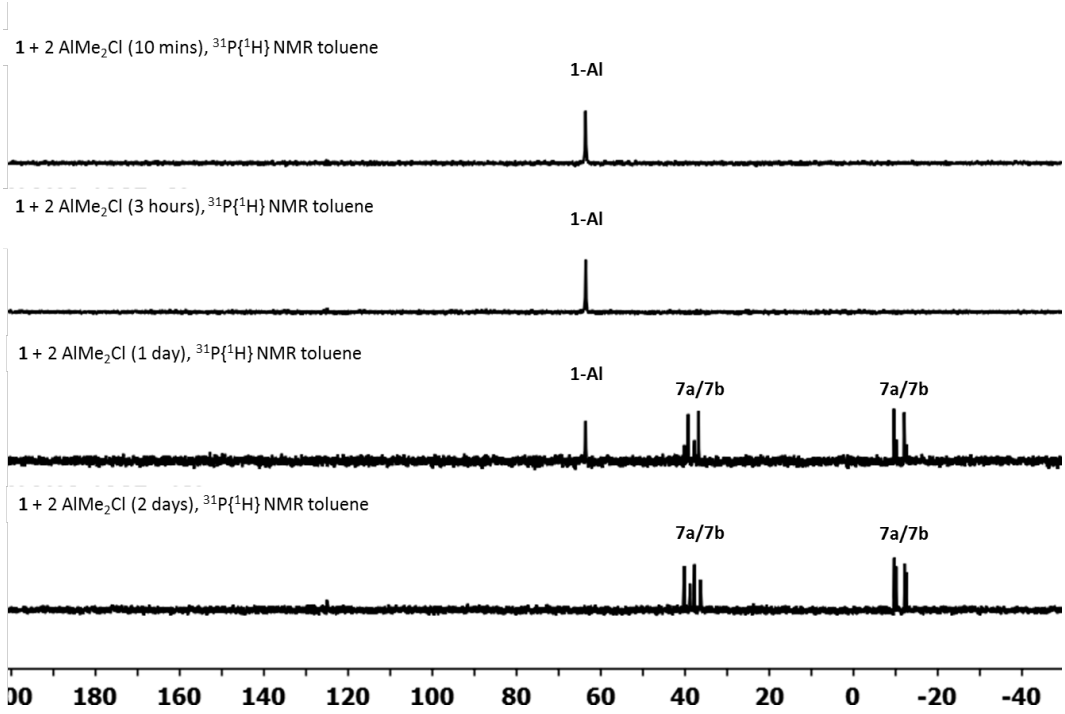

Figure S13. $^{31}P\{^{1}H\}$ NMR spectra of **1** + 2 $AlMe_2Cl$.

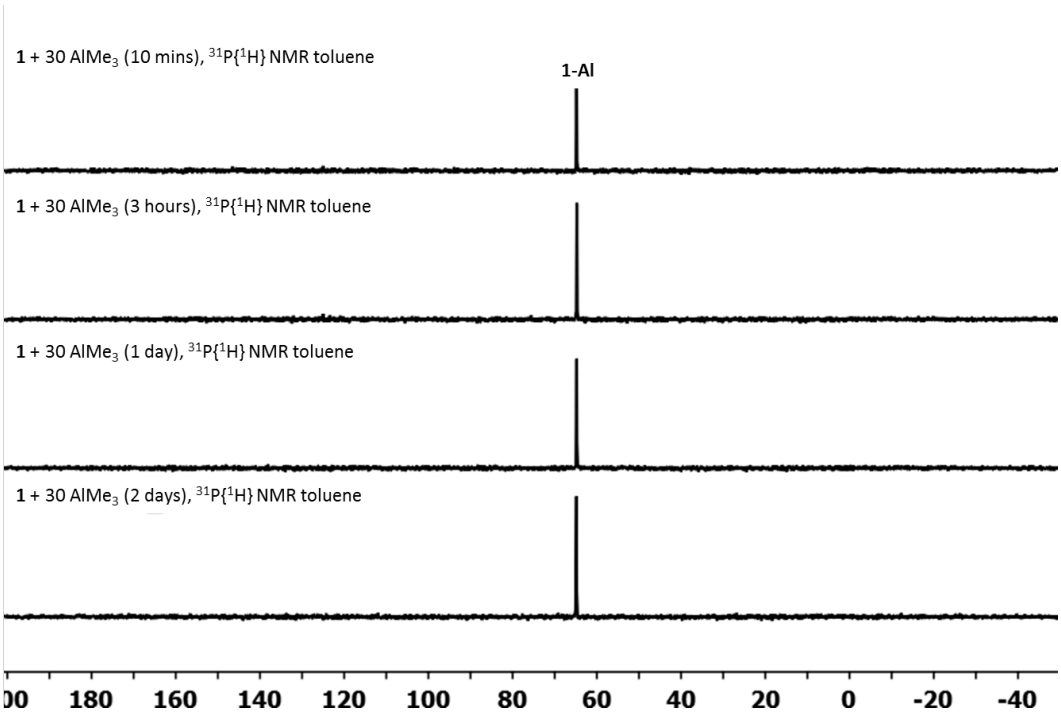

Figure S14. $^{31}P\{^{1}H\}$ NMR spectra of **1** + 30 $AlMe_3$.

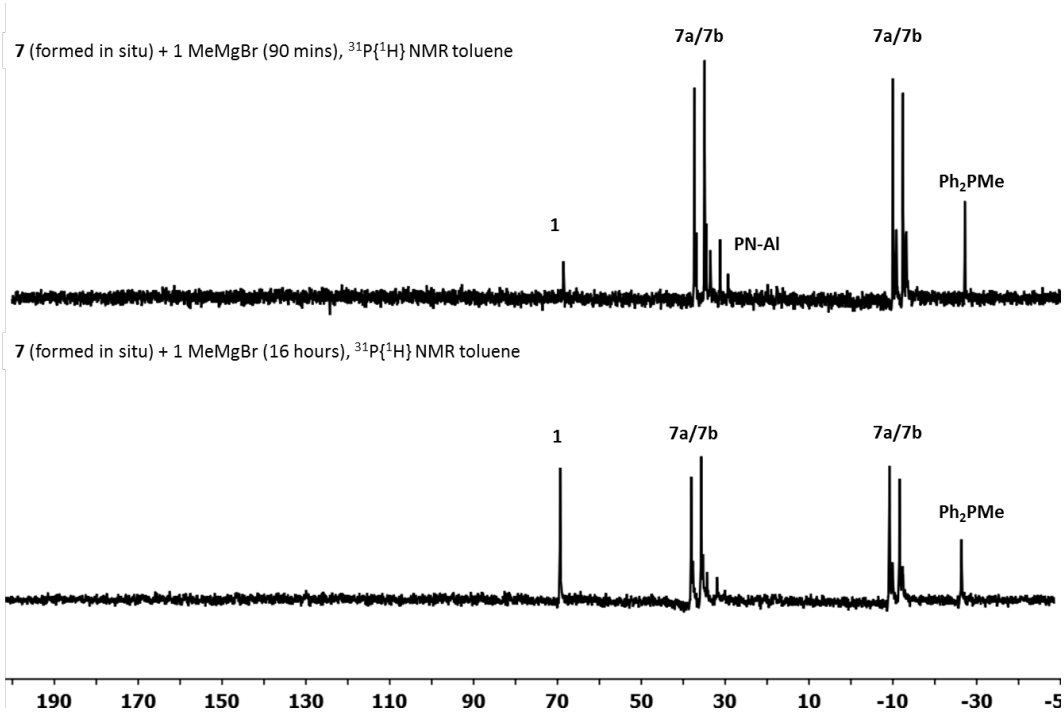

Figure S15. $^{31}P\{^{1}H\}$ NMR spectra of **7** (formed in situ) + MeMgBr.

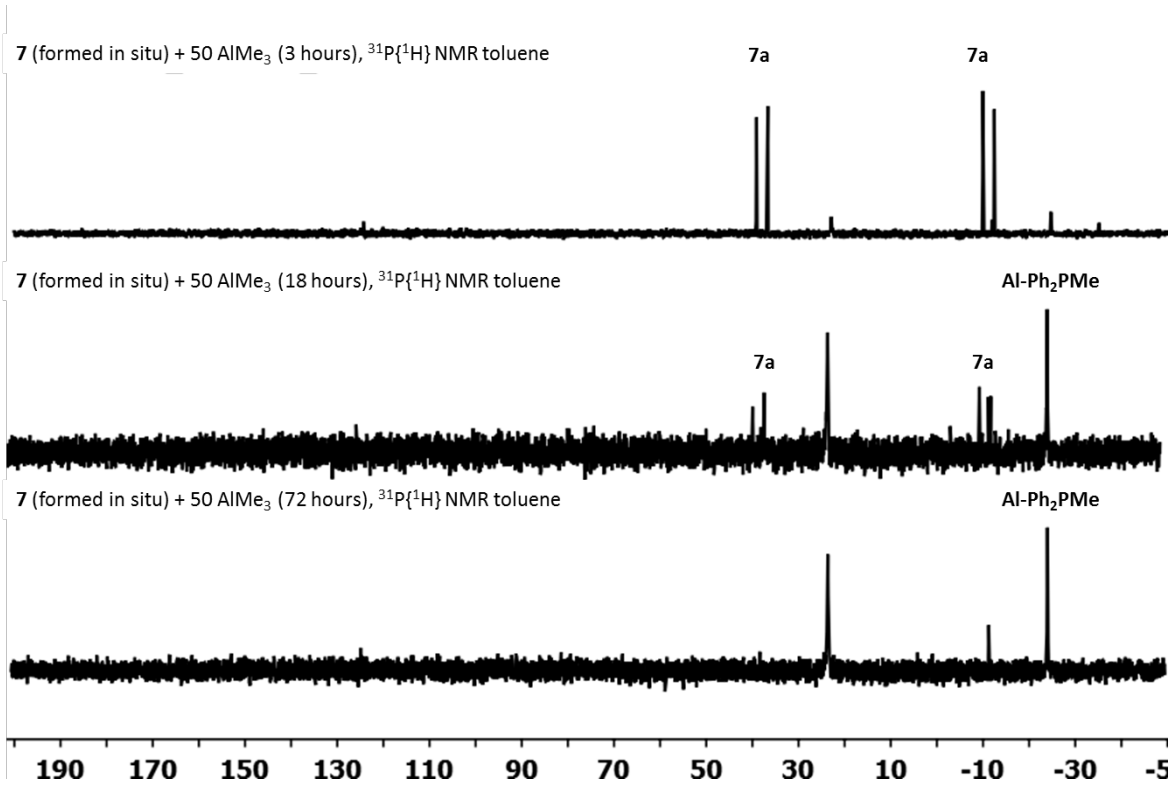

Figure S16. $^{31}P\{^{1}H\}$ NMR spectra of **7** (formed in situ) + 50 $AlMe_3$.

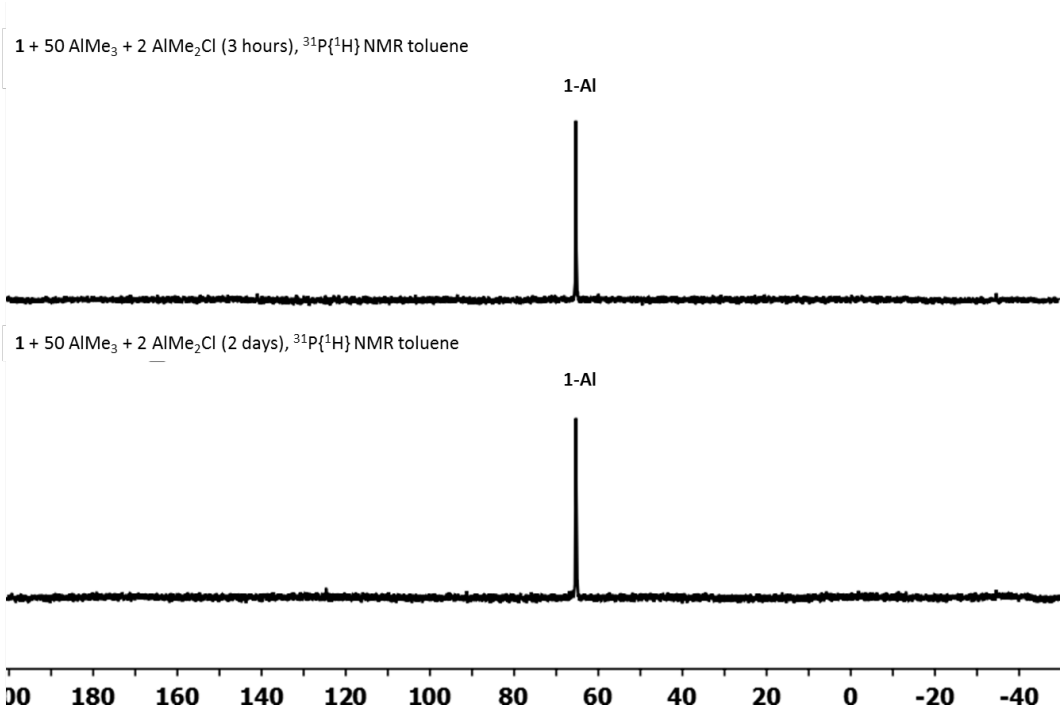

Figure S17. $^{31}P\{^{1}H\}$ NMR spectra of **1** + 50 $AlMe_3$, followed by 2 $AlMe_2Cl$.

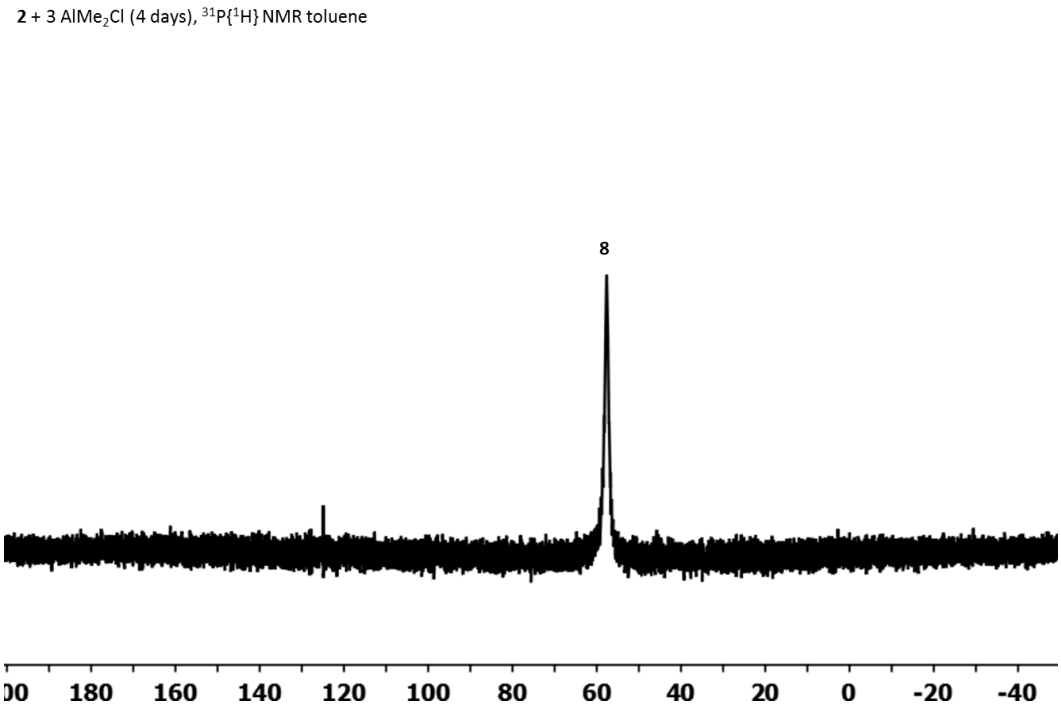

Figure S18. $^{31}P\{^{1}H\}$ NMR spectrum of **2** + 3 $AlMe_2Cl$.

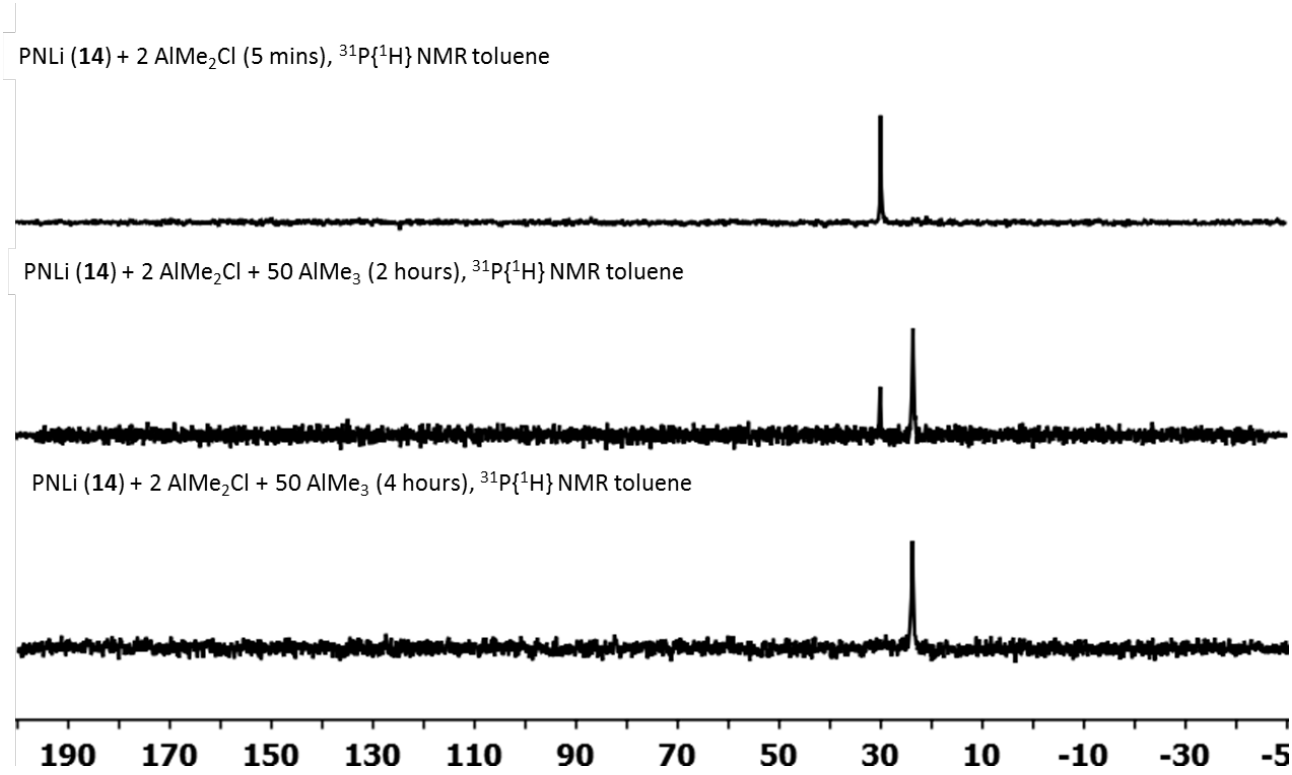

Figure S19. $^{31}P\{^{1}H\}$ NMR spectra of **14** + 2 $AlMe_2Cl$, followed by 50 $AlMe_3$.

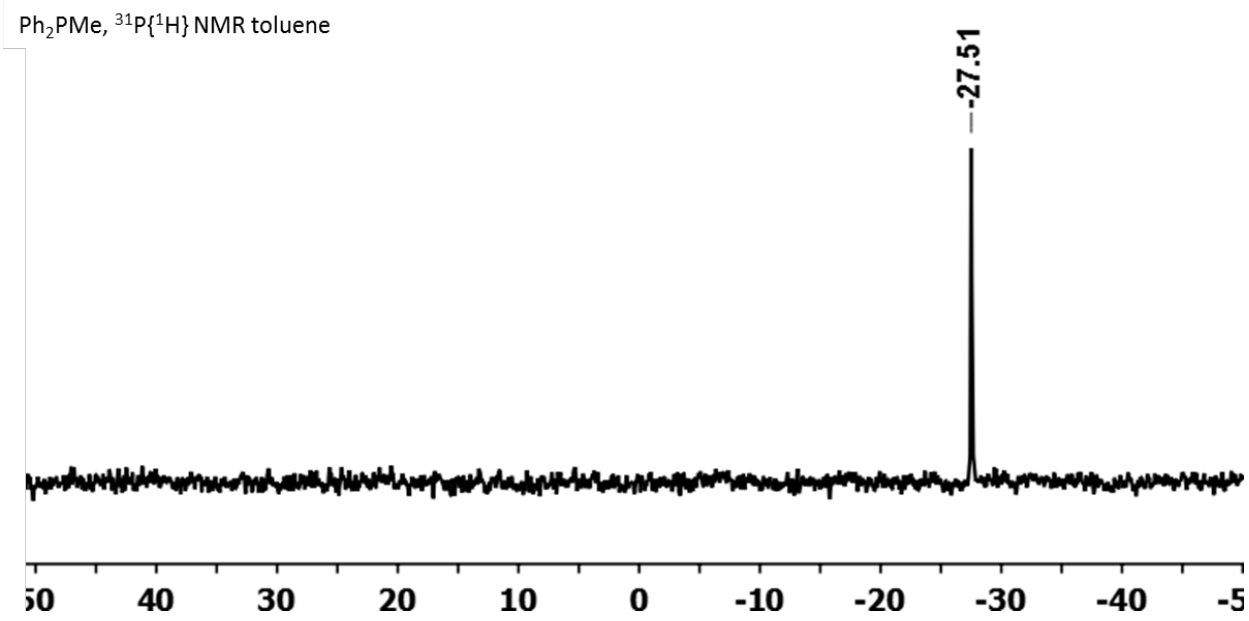

Figure S20. $^{31}P\{^{1}H\}$ NMR spectrum of Ph_2PMe.

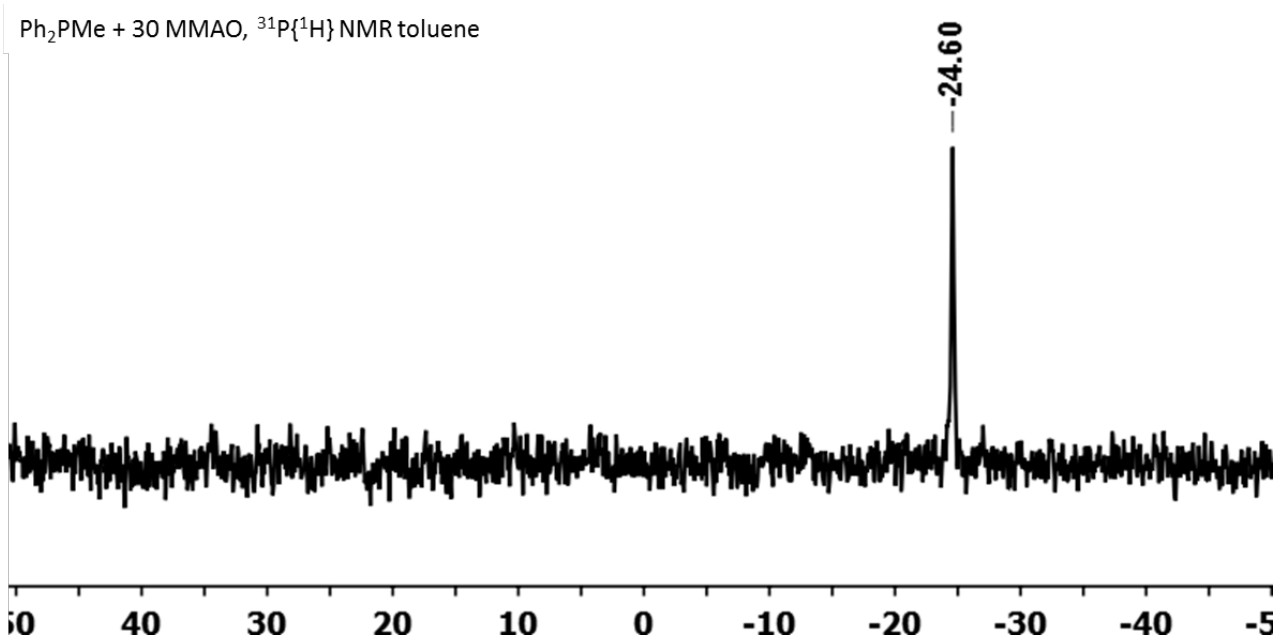

Figure S21. $^{31}P\{^{1}H\}$ NMR spectrum of Ph_2PMe + 30 MMAO.

Computational

DFT calculations were performed using Gaussian 09 Revision C.01.[5] The initial coordinates for the PNP and PPN moieties were extracted from the crystallographic coordinates from the solid-state structures of complexes **3** and **7**. The P and N substituents were substituted for protons (**Figure 7**) or for methyl groups (**Figure S22**). The geometries were optimized without restraint using the 6-311+G(d,p) basis set and B3LYP-hybrid functional. The resulting geometries was confirmed as absolute energetic minima via frequency calculations that did not yield imaginary vibrations < -10 cm^{-1}. The calculated electrostatic potentials were mapped, using GaussView, onto the 0.04 $e^-/Å^3$ electron density isosurface. Red regions indicate potential density below or equal to the minimum set limit and blue indicates potential density above or equal to the maximum set limit (see scale).

In both theoretical models of the PPN and PNP isomers, either with H or methyl substituents, it was found that isomerization to PPN is accompanied by significant accumulation of electron density potential around the N atom. The truncated theoretical models of the PNP frameworks show that, in this isomer, the electron density is instead more localized around the ligating P atoms.

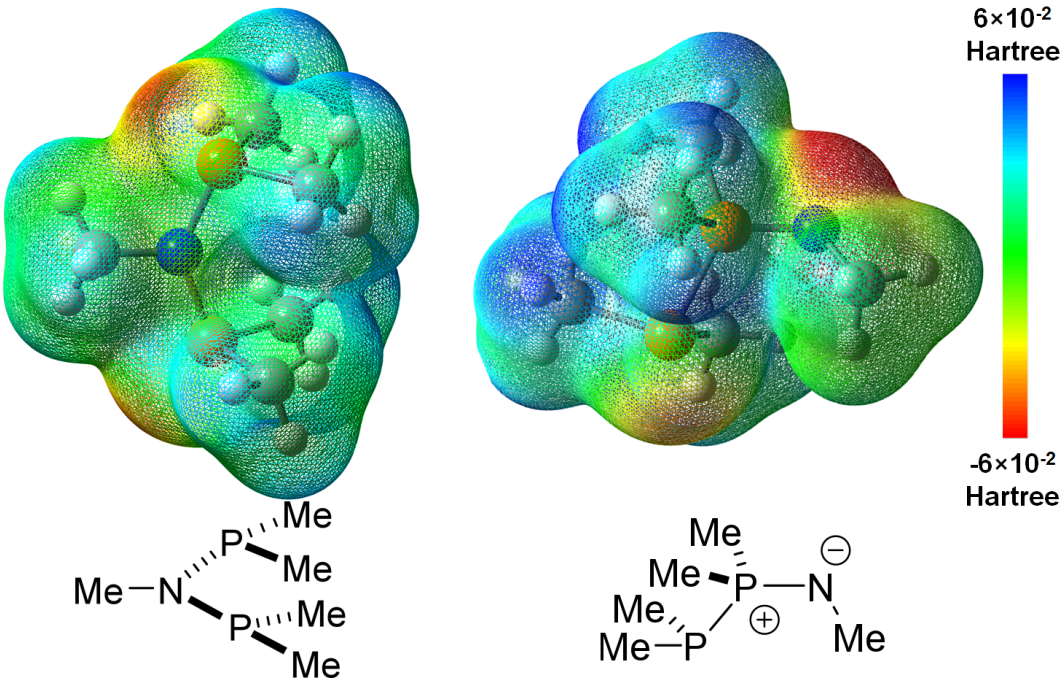

Figure S22. Electrostatic potential mapped onto electron density isosurfaces (isovalue = 0.004 $e^-/Å^3$) of model $PMe_2NMePMe_2$ (left) and isomerized PMe_2PMe_2NMe (right).

Crystallography

Table S1. Crystal and Refinement Data for Complexes **3**, **4**, and **7**.

Compound	**3**	**4**	**7b/7c**
CCDC	1471532	1471534	1471530
Empirical formula	$C_{33}H_{31}Cl_7CrNP_2$	$C_{30}H_{33}Cl_9CrNP_2$	$C_{31.82}H_{29.47}AlCl_{2.17}NP_2$
Formula weight	803.68	840.56	591.96
Temperature/K	100.02	100.01	99.99
Crystal system	triclinic	triclinic	triclinic
Space group	P-1	P-1	P-1
a/Å	10.8962(7)	13.5833(11)	11.6158(8)
b/Å	12.8113(15)	14.3977(14)	11.8725(10)
c/Å	13.8238(17)	20.235(2)	12.0068(11)
α/°	75.733(6)	94.594(5)	94.734(5)
β/°	81.438(5)	92.147(5)	100.951(5)
γ/°	73.265(5)	109.222(4)	110.634(5)
Volume/Å^3	1784.7(3)	3716.2(6)	1501.1(5)
Z	2	4	2
ρ_{calc}g/cm^3	1.496	1.502	1.310
μ/mm^{-1}	0.96	1.064	0.390
F(000)	818	1708	615
Crystal size/mm^3	0.21 × 0.17 × 0.12	0.28 × 0.15 × 0.11	0.25 × 0.20 × 0.10
Radiation	MoKα (λ = 0.71073)	MoKα (λ = 0.71073)	MoKα (λ = 0.71073)
2Θ range for data collection/°	5.032 to 72.636	4.802 to 80	3.502 to 72.55
Index ranges	-18 ≤ h ≤ 18, -21 ≤ k ≤ 21, -23 ≤ l ≤ 23	-24 ≤ h ≤ 24, -25 ≤ k ≤ 25, -35 ≤ l ≤ 35	-19 ≤ h ≤ 14, -19 ≤ k ≤ 19, -19 ≤ l ≤ 18
Reflections collected	112813	289169	24839
Independent reflections	17281 [R_{int} = 0.0544, R_{sigma} = 0.0426]	44225 [R_{int} = 0.0581, R_{sigma} = 0.0663]	13728 [R_{int} = 0.0500, R_{sigma} = 0.1081]
Data/restraints/parameters	17281/38/426	44225/0/837	12449/0/355
Goodness-of-fit on F^2	1.023	1.047	1.038
Final R indexes [I>=2σ (I)]	R_1 = 0.0383, wR_2 = 0.0770	R_1 = 0.0585, wR_2 = 0.1157	R_1 = 0.0708, wR_2 = 0.1878
Final R indexes [all data]	R_1 = 0.0636, wR_2 = 0.0852	R_1 = 0.1128, wR_2 = 0.1340	R_1 = 0.1405, wR_2 = 0.2275
Largest diff. peak/hole / e Å^{-3}	1.14/-1.25	1.11/-1.59	0.7/-1.63

Table S2. Crystal and Refinement Data for Complexes **8**, **10**$^{+}$**[AlCl$_4$]**$^{-}$, and **11**.

Compound	**8**	**10**$^{+}$**[AlCl$_4$]**$^{-}$	**11**
CCDC	1471529	1471528	1471531
Empirical formula	$C_{30}H_{36}Al_2Cl_3NP_2$	$C_{27}H_{28}AlCl_4NP_2$	$C_{30}H_{26}AlCl_3OP_2$
Formula weight	632.85	597.22	597.78
Temperature/K	100.02	99.99	100
Crystal system	triclinic	orthorhombic	monoclinic
Space group	P-1	$P2_12_12_1$	Pc
a/Å	10.5133(4)	10.2494(5)	9.3545(11)
b/Å	12.7230(5)	15.7035(8)	9.3024(11)
c/Å	13.7659(6)	17.8108(10)	17.270(2)
α/°	64.1950(10)	90	90
β/°	80.7120(10)	90	101.913(3)
γ/°	80.8120(10)	90	90
Volume/Å^3	1627.68(11)	2866.7(3)	1470.5(3)
Z	2	4	2
ρ_{calc}g/cm^3	1.291	1.384	1.35
μ/mm^{-1}	0.455	0.573	0.473
F(000)	660	1232	616
Crystal size/mm^3	0.26 × 0.22 × 0.15	0.23 × 0.16 × 0.15	0.48 × 0.22 × 0.16
Radiation	MoKα (λ = 0.71073)	MoKα (λ = 0.71073)	MoKα (λ = 0.71073)
2Θ range for data collection/°	4.878 to 61.076	3.458 to 61.082	4.378 to 75.408
Index ranges	-15 ≤ h ≤ 15, -18 ≤ k ≤ 18, -19 ≤ l ≤ 19	-14 ≤ h ≤ 14, -22 ≤ k ≤ 19, -25 ≤ l ≤ 25	-13 ≤ h ≤ 13, -13 ≤ k ≤ 13, -24 ≤ l ≤ 24
Reflections collected	73966	59918	61923
Independent reflections	9931 [R_{int} = 0.0345, R_{sigma} = 0.0222]	8770 [R_{int} = 0.0432, R_{sigma} = 0.0278]	9057 [R_{int} = 0.0376, R_{sigma} = 0.0243]
Data/restraints/parameters	9931/0/348	8770/0/322	9057/2/362
Goodness-of-fit on F^2	1.069	1.063	1.060
Final R indexes [I>=2σ (I)]	R_1 = 0.0394, wR_2 = 0.1096	R_1 = 0.0237, wR_2 = 0.0549	R_1 = 0.0304, wR_2 = 0.0793
Final R indexes [all data]	R_1 = 0.0485, wR_2 = 0.1145	R_1 = 0.0265, wR_2 = 0.0582	R_1 = 0.0364, wR_2 = 0.0823
Largest diff. peak/hole / e Å^{-3}	0.52/-1.48	0.43/-0.24	0.43/-0.27

Table S3. Crystal and Refinement Data for Complex **12**.

Compound	**12**
CCDC	1471533
Empirical formula	$C_{78.76}H_{78.28}AlCl_{6.24}Cr_2N_2P_4$
Formula weight	1528.95
Temperature/K	100
Crystal system	triclinic
Space group	P-1
a/Å	14.6582(5)
b/Å	22.7883(8)
c/Å	24.5404(9)
α/°	68.6350(10)
β/°	88.7120(10)
γ/°	88.3820(10)
Volume/Å^3	7630.3(5)
Z	4
ρ_{calc}g/cm^3	1.331
μ/mm^{-1}	0.642
F(000)	3168
Crystal size/mm^3	0.21 × 0.20 × 0.07
Radiation	MoKα (λ = 0.71073)
2Θ range for data collection/°	4.48 to 60.998
Index ranges	-20 ≤ h ≤ 20, -32 ≤ k ≤ 32, -35 ≤ l ≤ 35
Reflections collected	215976
Independent reflections	46404 [R_{int} = 0.0545, R_{sigma} = 0.0572]
Data/restraints/parameters	46404/2754/1727
Goodness-of-fit on F^2	1.074
Final R indexes [I>=2σ (I)]	R_1 = 0.0573, wR_2 = 0.1261
Final R indexes [all data]	R_1 = 0.0948, wR_2 = 0.1385
Largest diff. peak/hole / e Å^{-3}	1.42/-1.27

REFERENCES

(1) Jiang, T.; Zhang, S.; Jiang, X.; Yang, C.; Niu, B.; Ning, Y. *J. Mol. Catal. A: Chem.* **2008**, *279*, 90-93.
(2) Bollmann, A.; Blann, K.; Dixon, J. T.; Hess, F. M.; Killian, E.; Maumela, H.; McGuinness, D. S.; Morgan, D. H.; Neveling, A.; Otto, S.; Overett, M.; Slawin, A. M. Z.; Wasserscheid, P.; Kuhlmann, S. *J. Am. Chem. Soc.* **2004**, *126*, 14712-14713.
(3) Fei, Z.; Scopellitia, R.; Dyson, P. J. *Dalton Trans.* **2003**, 2772-2779.
(4) Barron A. R. *J. Chem. Soc. Dalton Trans.* **1988**, 3047-3050.
(5) Gaussian 09, Revision C.01, Frisch, M. J.; Trucks, G. W.; Schlegel, H. B.; Scuseria, G. E.; Robb, M. A.; Cheeseman, J. R.; Scalmani, G.; Barone, V.; Mennucci, B.; Petersson, G. A.; Nakatsuji, H.; Caricato, M.; Li, X.; Hratchian, H. P.; Izmaylov, A. F.; Bloino, J.; Zheng, G.; Sonnenberg, J. L.; Hada, M.; Ehara, M.; Toyota, K.; Fukuda, R.; Hasegawa, J.; Ishida, M.; Nakajima, T.; Honda, Y.; Kitao, O.; Nakai, H.; Vreven, T.; Montgomery, Jr., J. A.; Peralta, J. E.; Ogliaro, F.; Bearpark, M.; Heyd, J. J.; Brothers, E.; Kudin, K. N.; Staroverov, V. N.; Kobayashi, R.; Normand, J.; Raghavachari, K.; Rendell, A.; Burant, J. C.; Iyengar, S. S.; Tomasi, J.; Cossi, M.; Rega, N.; Millam, J. M.; Klene, M.; Knox, J. E.; Cross, J. B.; Bakken, V.; Adamo, C.; Jaramillo, J.; Gomperts, R.; Stratmann, R. E.; Yazyev, O.; Austin, A. J.; Cammi, R.; Pomelli, C.; Ochterski, J. W.; Martin, R. L.; Morokuma, K.; Zakrzewski, V. G.; Voth, G. A.; Salvador, P.; Dannenberg, J. J.; Dapprich, S.; Daniels, A. D.; Farkas, Ö.; Foresman, J. B.; Ortiz, J. V.; Cioslowski, J.; Fox, D. J. Gaussian, Inc., Wallingford CT, 2009.